A Simplified Rubber Model with Damage

Stefan Kolling [a], Paul A. Du Bois [b] & Dave J. Benson [c]

[a] DaimlerChrysler AG, EP/SPB, HPC X411, 71059 Sindelfingen, Germany
E-Mail: stefan.kolling@daimlerchrysler.com

[b] Consulting Engineer, Freiligrathstr. 6, 63071 Offenbach, Germany
E-Mail: paul.dubois@gmx.net

[c] University of California, Dept. of Mechanical and Aerospace Engineering, San Diego, USA
E-Mail: dbenson@ucsd.edu

Abstract:
Simulation of rubber-like materials is usually based on hyperelasticity. If strain-rate dependency has to be considered viscous dampers also have to be taken into account in the rheological model. A disadvantage of such a material model is time-consuming parameter identification associated with the damping constants. With MAT_SIMPLIFIED_RUBBER (Material no. 181), a material law is implemented in LS-DYNA which allows fast generating of input data based on uniaxial static and dynamic tensile tests at different strain rates. However, unloading, i.e. forming of a hysteresis, cannot be modeled easily using Mat181. Thus, an extension of Mat181 based on a damage formulation was desirable.
In this paper, we show the theoretical background and algorithmic setup of our model which has been implemented as MAT_SIMPLIFIED_RUBBER_WITH_DAMAGE (Material no. 183) in LS-DYNA. As an application, the validation of a soft and a hard rubber under loading and subsequent unloading at different strain rates is shown.

Keywords:

Material Modelling, Rubber, Hyperelasticity, Strain-rate Dependency, Elastic Damage, Explicit Finite Element Method

1 Material law formulation

1.1 Basic equations

The most straight forward generalization of Hooke's law to large displacements and large deformations is hyperelasticity, see [9], [10]. A hyperelastic material is path independent and allows to calculate the second Piola-Kirchhoff stress tensor $\mathbf{S} = 2\partial W / \partial \mathbf{C}$ from a derivative of the energy functional $W = \hat{W}(\mathbf{C})$ with respect to the components of the right Cauchy-Green strain tensor $\mathbf{C} = \mathbf{F}^T\mathbf{F}$, where $\mathbf{F} = \mathrm{Grad}\,\mathbf{x}$ is the deformation gradient. In LS-DYNA we can distinguish two families of hyperelastic materials. The first one is based on an energy functional expressed in the invariants of the right Cauchy-Green tensor: $W = \hat{W}(I_C, II_C, III_C)$. The invariants of $\mathbf{C}$ are given by $I_C = \mathbf{1} : \mathbf{C} = \mathrm{tr}\,\mathbf{C}$, $II_C = \frac{1}{2}\left(I_C^2 - \mathbf{C} : \mathbf{C}\right)$ and $III_C = \det \mathbf{C}$. Then, the derivative yields

$$\mathbf{S} = 2\frac{\partial W}{\partial I_C}\mathbf{1} + 2\frac{\partial W}{\partial II_C}\left(I_C\mathbf{1} - \mathbf{C}\right) + 2\frac{\partial W}{\partial III_C}III_C\mathbf{C}^{-1}. \tag{1}$$

The Cauchy stress $\boldsymbol{\sigma}$ can now be obtained by forming $\boldsymbol{\sigma} = J^{-1}\mathbf{F}\mathbf{S}\mathbf{F}^T$, where $J = \det \mathbf{F}$ is the relative volume.

The second family of hyperelastic materials is formulated in terms of principle stretch ratios. Therefore, it is instructive to rewrite the former expressions in terms of principal stretches λ_i. After a decomposition $\mathbf{F} = \mathbf{R}\mathbf{U}$, where $\mathbf{R}^T\mathbf{R} = \mathbf{1}$ and $\mathbf{U} = \mathbf{U}^T$, the invariants are given by $I_C = \lambda_1^2 + \lambda_2^2 + \lambda_3^2$, $II_C = \lambda_1^2\lambda_2^2 + \lambda_2^2\lambda_3^2 + \lambda_3^2\lambda_1^2$, $III_C = \lambda_1^2\lambda_2^2\lambda_3^2 = J^2$ and the Cauchy stress $\boldsymbol{\sigma}$ and the principal engineering stress $\boldsymbol{\tau}$ can be obtained as

$$\sigma_i = \frac{1}{\lambda_j\lambda_k}\frac{\partial W}{\partial \lambda_i} \Rightarrow \lambda_j\lambda_k\sigma_i =: \tau_i = \frac{\partial W}{\partial \lambda_i}. \tag{2}$$

An overview of hyperelastic laws which are implemented in LS-DYNA is given in Table 1, see also references [1]-[6] and [8].

Law	Keyword
7	MAT_BLATZ-KO_RUBBER
2	MAT_ORTHOTROPIC_ELASTIC
33	MAT_FRAZER-NASH_RUBBER
27	MAT_MOONEY-RIVLIN_RUBBER
38	MAT_BLATZ-KO_FOAM
83	MAT_FU_CHANG_FOAM
127	MAT_ARRUDA_BOYCE_RUBBER
181	MAT_SIMPLIFIED_RUBBER
183	MAT_SIMPLIFIED_RUBBER_WITH_DAMAGE

Table 1: Overview of hyperelastic materials in LS-DYNA.

A hyperelastic law formulated in terms of principle stretches is given by Ogden:

$$W = \sum_{i=1}^{3}\sum_{j=1}^{n}\frac{\mu_j}{\alpha_j}\left(\lambda_i^{*\alpha_j} - 1\right) + K(J - 1 - \ln J) \Rightarrow \sigma_i = \sum_{p=1}^{n}\frac{\mu_p}{J}\left[\lambda_i^{*\alpha_p} - \sum_{k=1}^{3}\frac{\lambda_k^{*\alpha_p}}{3}\right] + K\frac{J-1}{J}. \tag{3}$$

Here, α_j are non-integer, $J = \lambda_1\lambda_2\lambda_3$ and $\lambda_i^* = \lambda_i J^{-1/3}$. Note that the penalty term corresponds to a purely hydrostatic stress and, therefore, the deviatoric part of the Ogden functional generates a zero stress in the undeformed configuration. In LS-DYNA, a tabulated version of the Ogden material law has been implemented with the material law MAT_SIMPLIFIED_RUBBER. Here, the Ogden functional (3) is internally determined from the uniaxial engineering stress-strain curve by defining a tabulated function of the principal stretch ratio as follows [7]:

$$f(\lambda)=\sum_{p=1}^{n}\mu_p\lambda^{*\alpha_p} \quad \Rightarrow \quad \sigma_i=\frac{1}{J}\left(f(\lambda_i)-\frac{1}{3}\sum_{j=1}^{3}f(\lambda_j)\right)+K\frac{J-1}{J}. \tag{4}$$

1.2 Damage formulation

In rubbers the measured quasistatic loading and unloading paths are not necessarily identical. Consequently the material cannot be considered to be hyperelastic during unloading and subsequent reloading: the rubber has a path-dependent behaviour and a one-to-one correspondence between stress and strain no longer exists. The current development uses a damage formulation to simulate the rubber behaviour under cyclic loading. The implementation is limited at first to the incompressible Ogden functional for the simulation of natural rubbers. The Ogden functional is written as

$$W=\left(1-d\left(\frac{W_0}{W_{0,\max}}\right)\right)\sum_{i=1}^{3}\sum_{j=1}^{n}\frac{\mu_j}{\alpha_j}\left(\lambda_i^{*\alpha_j}-1\right)+U(J). \tag{5}$$

As can be seen in the formula above, the damage parameter d is considered to be a function of the elastic deviatoric energy and the maximum of the elastic deviatoric energy over the deformation path :

$$\begin{aligned} W_0 &= \sum_{i=1}^{3}\sum_{j=1}^{n}\frac{\mu_j}{\alpha_j}\left(\lambda_i^{*\alpha_j}-1\right) \\ W_{0,\max} &= \max\left(W_0, W_{0,\max}\right) \Rightarrow 0 \le \frac{W_0}{W_{0,\max}} \le 1 \Rightarrow 0 \le d \le 1 \end{aligned} \tag{6}$$

The principal true stresses can no longer be computed directly from the energy functional since due to the damage the material has become path-dependent and a one-to-one relationship between stress and strain no longer exists. However by using the second law of thermodynamics an expression for the principal true stresses can still be obtained:

$$W=\left(1-d\left(\frac{W_0}{W_{0,\max}}\right)\right)\sum_{i=1}^{3}\sum_{j=1}^{n}\frac{\mu_j}{\alpha_j}\left(\lambda_i^{*\alpha_j}-1\right)+U(J) \Rightarrow \begin{cases} \sigma_i \neq \dfrac{1}{\lambda_j\lambda_k}\dfrac{\partial W}{\partial \lambda_i} \\ \sigma_i = (1-d)\dfrac{1}{\lambda_j\lambda_k}\dfrac{\partial W_0}{\partial \lambda_i}+\dfrac{1}{\lambda_j\lambda_k}\dfrac{\partial U}{\partial \lambda_i} \end{cases} \tag{7}$$

It is thus sufficient to compute the undamaged stress values and multiply the deviatoric part by (1-d). The function d is tabulated and only the abscissa needs to be computed in order to perform the table lookup. For more details concerning the damage formulation we refer to [13].

2 Numerical treatment

2.1 Implementation

Our implementation is a generalisation of the incompressible module in MAT_181 [7] including a damage formulation to simulate the unloading of rubber materials. Hysteresis could only be simulated in MAT_181 by using rate effects to fit the unloading curve. This can be cumbersome. Specific to our formulation is that the function d of the energy function will be tabulated in such a way that a measured unloading path from testing is exactly reproduced in the simulation. It is therefore necessary to provide a closed-loop measurement in terms of engineering stress/strain resulting from a uniaxial tensile (or compressive) test in input (see Figure 1).

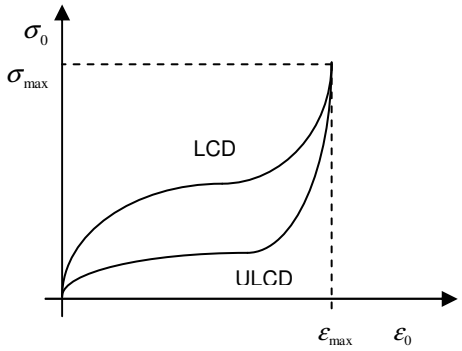

Figure 1: Definition of load curve

In Figure 1, LCD is a load curve giving the loading branch of the closed loop and ULCD is a load curve giving the unloading branch. It is important that both load curves form a closed loop: maximum stress and maximum strain must be identical for both load curves. In our current implementation, the unloading curve is defined in tension as well as in compression resulting in 2 closed loops. This allows defining a different damage evolution in tension and compression if corresponding test data are available. If no damage is considered (ULCD=0) the original incompressible version of MAT_181 is recovered. The function d is now internally computed from the input curves LCD and ULCD, here we make the assumption of incompressibility: J=1 and U=0:

$$
\begin{aligned}
&W_{0,\max} = V_0 \int_0^{\varepsilon_{\max}} \sigma_{0,lcd}\, d\varepsilon_0 = \int_0^{\varepsilon_{\max}} \sigma_{0,lcd}\, d\varepsilon_0 \\
&W_0(\varepsilon_0) = \int_0^{\varepsilon_0} \sigma_{0,lcd}\, d\varepsilon_0 \\
&d\left(\frac{W_0(\varepsilon_0)}{W_{0,\max}}\right) = 1 - \frac{\sigma_{ulcd}(\varepsilon_0)}{\sigma_{lcd}(\varepsilon_0)}
\end{aligned}
\qquad (8)
$$

This allows to tabulate the damage parameter d as a function of the energy ratio. This is done during the initialisation of the problem. For every explicit timestep, the energy ratio must be computed. For that purpose we determine the uniaxial energy function from the quasistatic load curve (use the stress-strain curve from the table with lowest strain rate):

$$
\begin{aligned}
&\sigma_0(\varepsilon_0) \text{ is tabulated in input} \\
&\lambda = \varepsilon_0 + 1 \\
&W_u(\lambda) = \int_0^{\varepsilon_0} \sigma_0 d\varepsilon_0 = \int_0^{\lambda} \sigma_0 d\lambda = W_u(\varepsilon_0)
\end{aligned}
\qquad (9)
$$

This gives the energy function value for any longitudinal strain under uniaxial loading (tension and compression must be covered) Now we specifically evaluate the deviatoric part of the Ogden function

$$W = \sum_{i=1}^{3} \sum_{j=1}^{n} \frac{\mu_j}{\alpha_j}\left(\lambda_i^{*\alpha_j} - 1\right) + U(J) \qquad (10)$$

for uniaxial load conditions. With

$$\lambda_j = \lambda_k \approx \lambda_i^{-1/2}, \quad J \approx 1, \quad \lambda_j^* = \lambda_k^* \approx \lambda_i^{*-1/2} \qquad (11)$$

we obtain

$$W_{0,u}(\lambda_i) = \sum_{j=1}^{n} \frac{\mu_j}{\alpha_j}\left(\lambda_i^{*\alpha_j} - 1\right) + 2\sum_{j=1}^{n} \frac{\mu_j}{\alpha_j}\left(\lambda_i^{*-\alpha_j/2} - 1\right) \tag{12}$$

and

$$W_{0,u}\left(\lambda_i^{-1/2}\right) = \sum_{j=1}^{n} \frac{\mu_j}{\alpha_j}\left(\lambda_i^{*-\alpha_j/2} - 1\right) + 2\sum_{j=1}^{n} \frac{\mu_j}{\alpha_j}\left(\lambda_i^{*\alpha_j/4} - 1\right). \tag{13}$$

We can now define and compute an Ogden function for the energy analogously to the procedure followed in [7] for the stress:

$$\begin{aligned} g\left(\lambda_i^*\right) &= \sum_{j=1}^{n} \frac{\mu_j}{\alpha_j}\left(\lambda_i^{*\alpha_j} - 1\right) \\ g\left(\lambda_i^*\right) &= W_u(\lambda_i) - 2W_u\left(\lambda_i^{-1/2}\right) + 4W_u\left(\lambda_i^{1/4}\right) - \ldots \end{aligned} \tag{14}$$

2.2 Algorithmic setup

Using the equations derived in the last section, the damage algorithm then becomes as follows:

Step 1: calculate principal stretch ratios and engineering strains:

$$\varepsilon_{0i} = \lambda_i - 1 \tag{15}$$

Step 2: evaluate the Ogden functions for every stretch ratio:

$$\begin{aligned} f\left(\lambda_i^*\right) &= \lambda_i \sigma_0(\varepsilon_{0i}) + \sum_{n=1}^{\infty} \lambda_i^{(-1/2)^n} \sigma_0\left(\lambda_i^{(-1/2)^n} - 1\right) \\ g\left(\lambda_i^*\right) &= W_u(\varepsilon_{0i}) + \sum_{n=1}^{\infty} (-2)^n W_u\left(\lambda_i^{(-1/2)^n} - 1\right) \\ for\_ : \_ &\left|\lambda_i^{(-1/2)^n} - 1\right| \le 0.01 \end{aligned} \tag{16}$$

Step 3: calculate undamaged true stresses and deviatoric energies:

$$\begin{aligned} \sigma_i &= \frac{1}{J}\left(f\left(\lambda_i^*\right) - \frac{1}{3}\sum_{j=1}^{3} f\left(\lambda_j^*\right)\right) + K\frac{J-1}{J} \\ W_0 &= \sum_{i=1}^{3} g\left(\lambda_i^*\right) \end{aligned} \tag{17}$$

Step 4: compute the damage from the tabulated function and scale the stresses:

$$\begin{aligned} W_{0,\max} &= \max\left(W_{0,\max}, W_0\right) \\ d &= d\left(\frac{W_0}{W_{0,\max}}\right) \\ \sigma_i &= (1-d)(\sigma_i + p) - p \end{aligned} \tag{18}$$

3 Validation

Two rubber materials have been tested experimentally at the Ernst Mach Institute (EMI) in Freiburg/Germany for validation of the numerical model. The experimental setup depends on the load

direction. For compression tests, the setup consists of two pressure plates with the cube-like rubber specimen (6x6x6mm) in between. The lower pressure plate is supported by a load cell. For tensile tests, the specimen is fixed additionally by gluing to the pressure plates, see left hand side of Figure 2. Compression tests with unloading on rubber cubes were performed for a hard (shore 70) and a weak (shore 55) rubber, see right hand side of Figure 2. Moreover, dynamic tensile tests at different strain rates (0.01/s, 1/s and 100/s) without unloading were also realised for validation.

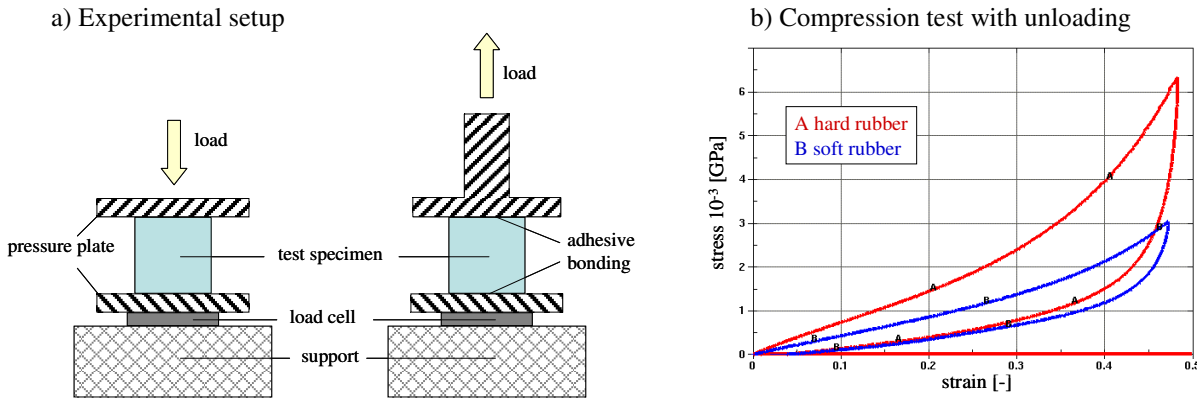

Figure 2: Experimental setup and data of compression test

In Figure 3, the results of the simulation are depicted. Since test data of the tension test with unloading was not available, damage is assumed similar to compressive side. As can be seen, the experimental data can be fitted exactly. As input data, the closed loop of the hysteresis in Figure 2 has been used directly in Mat_183.

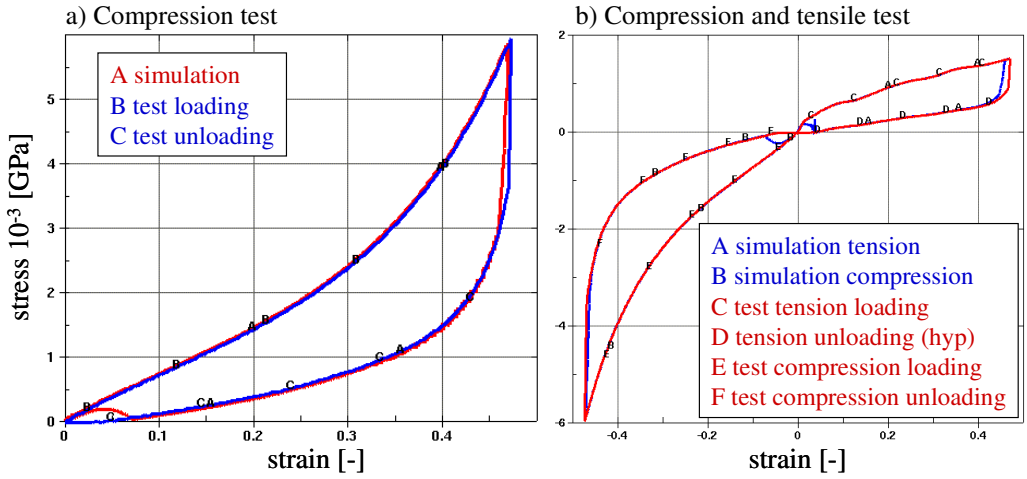

Figure 3: Simulation of loading and unloading (hard rubber)

In Figure 4, the simulation of the compressive test with unloading for the hard rubber is shown. Additionally, we chose different maximum compressions to demonstrate how the material law works if we leave the range of defined data points. As input data, we defined the closed loop (LCD and ULCD in Figure 1) given for maximum compression of 47.25%. In Figure 4a), we stay below this maximum compression and go up to 40%. The loading path can be simulated, of course, exactly. However, the unloading is an assumption: it is affine to the unloading path for 47.25% and after a certain time it is even congruent. Although it is purely an assumption, from an engineering point of view, we detect a healthy numerical behaviour of the material response. For the maximum compression of 47.25% in Figure 4b), we obtain the exact curve as given in the input data. What happens for higher compressions can be seen in Figure 4c) and d). The loading path is given as defined in the input according to extrapolation of the curves. The unloading path is, again, given numerically by the definition of the damage in the closed loop.

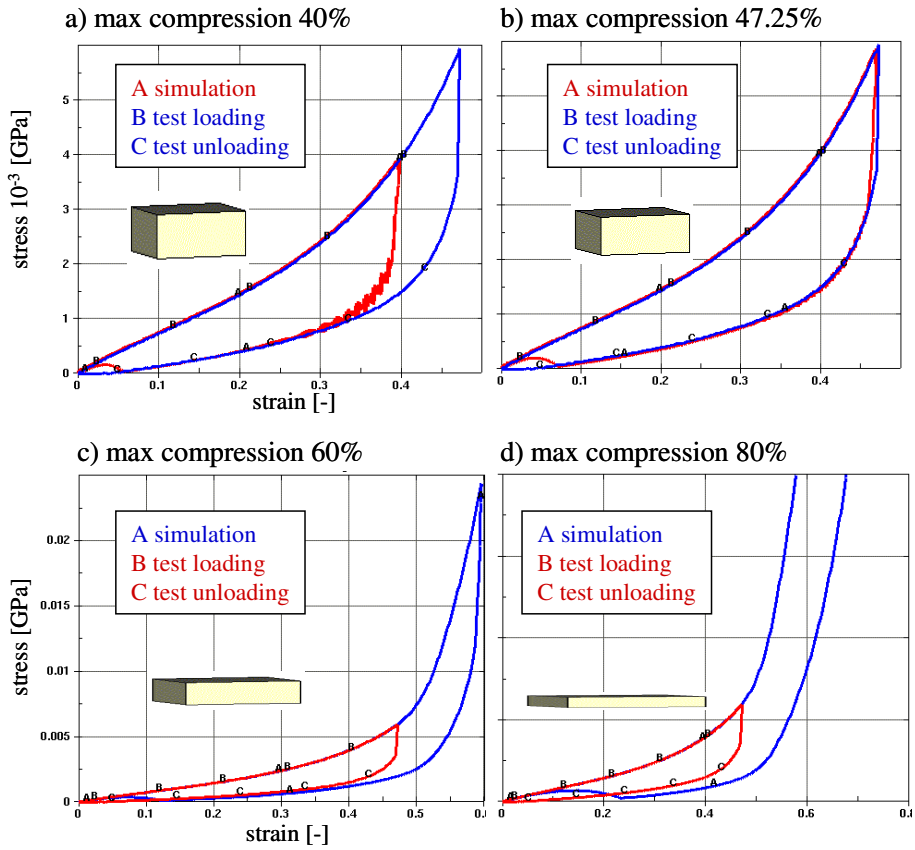

Figure 4: Compressive test (hard rubber) with unloading for different maximum compressions

Next, we compare the material laws MAT_SIMPLIFIED_RUBBER and its extension with damage MAT_SIMPLIFIED_RUBBER_WITH_DAMAGE. First some remarks concerning LS-DYNA 9.71 and higher:

- MAT_SIMPLIFIED_RUBBER_WITH_DAMAGE is available also for strain rate dependent materials, i.e. the load curve can be replaced by a table definition referring to the load curves at different strain rates.
- MAT_SIMPLIFIED_RUBBER has an extension with a damage model. This is, however, intended for the simulation of failure rather than for the simulation of unloading!

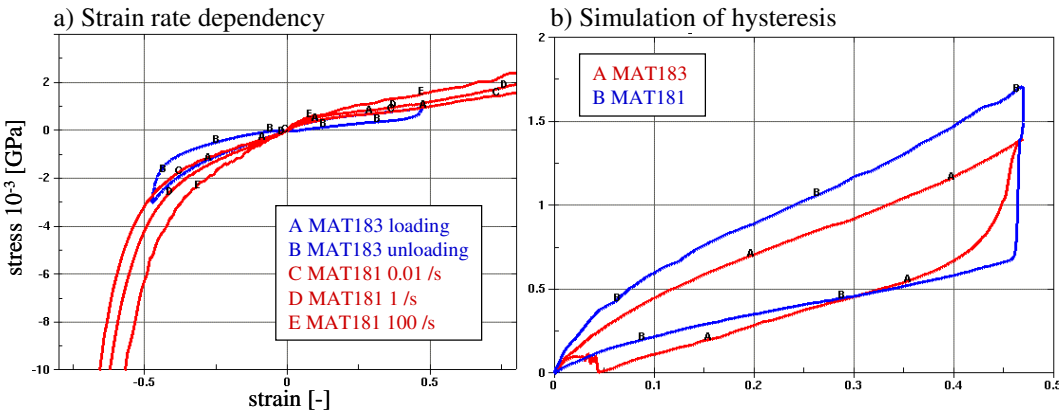

Figure 5: Comparison MAT_183 and MAT_181

For the simulation of a hysteresis loop, MAT_SIMPLIFIED_RUBBER can be used if the unloading is determined by the definition of the strain rate. In Figure 5a), the exact curves simulating the experiment are depicted. In Figure 5b), the strain rate sensitivity is artificially increased to obtain a

hysteresis loop in the quasi static case. Note that in this case, the material response for higher strain rates may be not exact anymore.
In our last validation example, we simulate the strain rate dependency of the soft rubber again in single element tensile tests with unloading. In Figure 6, we compare the material response of MAT181 and MAT183. For each material two tensile loads (with and without rate effects) are simulated resulting in the same maximum deformation. We then perform the analyses twice to illustrate the effect of different settings of the unloading flag TENSION. For TENSION=-1 (Figure 6a), rate effects are considered in the loading phase only. Consequently, the unloading path follows the quasistatic curve in MAT_181 and dynamic and quasistatic unloading paths are identical in MAT_183. For TENSION =1 (Figure 6b) rate effects are considered in loading and unloading phase. Loading and unloading path are then identical for MAT_181 resulting in a potentially unstable material model. With MAT_183 the unloading paths show rate dependency and (due to the damage formulation) are always below the loading path. The advantages of MAT_183 upon unloading are clear:

- rate effects can be considered
- damage formulation ensures energy dissipation and hence numerical stability

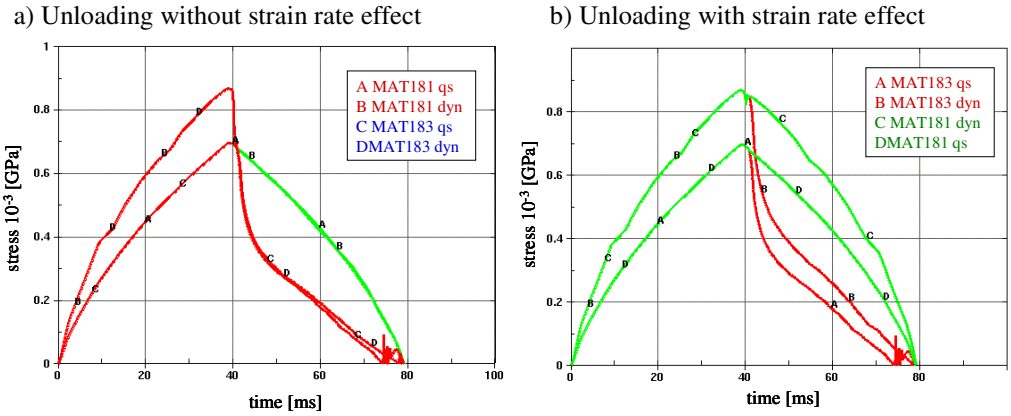

Figure 6: Comparison MAT_183 and MAT_181

In Figure 7, tensile tests with and without rate effects are again considered for MAT_183 only. This time different maximum deflections (corresponding to different strain rates upon loading) are applied. It is shown again that for TENSION=-1, quasistatic and dynamic unloading path coincide whereas for TENSION=1, rate effects are clearly present also upon unloading.

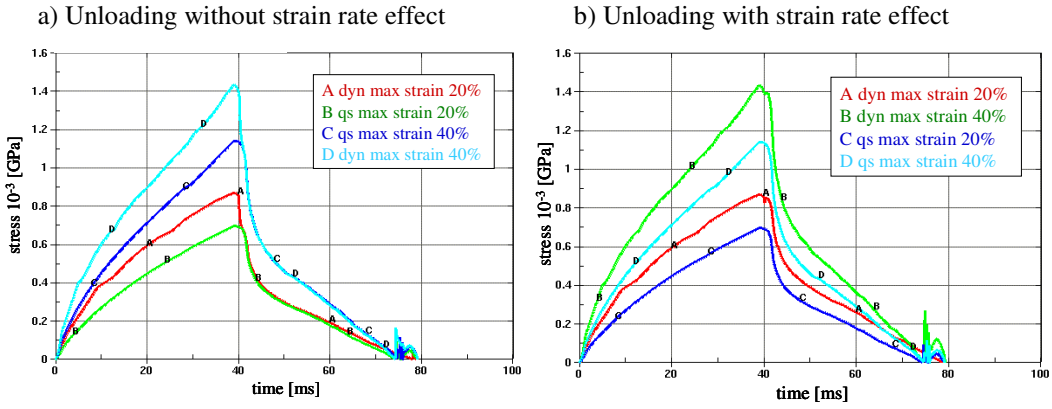

Figure 7: Strain-rate dependency using MAT_183

4 Summary

With the presented material formulation, exact simulation of test data for different strain rates in tension and compression can be achieved without any parameter fitting. Furthermore, stable and realistic unloading behaviour with energy dissipation is obtained based on a solid theoretical basis. The implementation has been done for solid and shell elements and is currently limited to the nearly incompressible case (Ogden functional). In the near future the damage formulation will be made available for the general hyperelastic formulation (Hill functional) also.

5 References

[1] J.O. Hallquist: LS-DYNA, Theoretical Manual, Livermore Software Technology Corporation, Report 1018, 1991.
[2] P.A. Du Bois: Crashworthiness Engineering Course Notes, Livermore Software Technology Corporation, 2004.
[3] P.J. Blatz & W.L. Ko: Application of finite elastic theory to the deformation of rubbery materials. Trans. Soc. Rheol., 6: 223-251, 1962.
[4] M. Mooney: A theory of large elastic deformations. J. Appl. Physics, 11:582-592, 1940.
[5] R.S. Rivlin: Large elastic deformations of isotropic materials. Proc. Roy. Soc. London, 241: 379-397, 1948.
[6] R.W. Ogden: Large deformation isotropic elasticity: on the correlation of theory and experiment for incompressible rubberlike solids. Proc. Roy. Soc. London, 326: 565-584, 1972.
[7] P.A. Du Bois: A simplified approach for the simulation of rubber-like materials under dynamic loading. 4th European LS-DYNA Users Conference, pp. D-I-31/46, 2003.
[8] P.A. Du Bois, W. Fassnacht & S. Kolling: General aspects of material models in LS-DYNA. LS-DYNA Forum, Bad Mergentheim, Germany 2002, V2:1-55.
[9] R. Hill: Aspects of invariance in solid mechanics. *Adv. Appl. Mech.* 18: 1–75, 1978.
[10] B. Storåkers: On material representation and constitutive branching in finite compressible elasticity. J. Mech. Phys. Solids, 34(2): 125-145, 1986.
[11] P.A. Du Bois, S. Kolling, M. Koesters & T. Frank: Material modeling of polymeric materials in crashworthiness analysis. 3rd Workshop for Material and Structural Behaviour at Crash Processes (*crash*MAT), Freiburg, Germany 2004.
[12] P. A. Du Bois, S. Kolling & T. Frank: Material behaviour of polymers under impact loading. International Symposium on crashworthiness of light-weight automotive structures, Trondheim, Norway, 2004. To appear at the International Journal of Impact Mechanics.
[13] Timmel, M.; Kaliske, M.; Kolling, S.: Modellierung gummiartiger Materialien bei dynamischer Beanspruchung. LS-DYNA Forum, Bamberg, Germany 2004, C-I-1/11.

